

Morphological Gradient Applied to New Active Contour Model for Color Image Segmentation

Nguyen Tran Lan Anh
Chonnam National University
300 Yongbong-Dong street, Bukgu
500-757, Gwangju, Korea
(82) 62-530-0147
ntlanh@hotmail.com

Young-Chul Kim
Chonnam National University
300 Yongbong-Dong street, Bukgu
500-757, Gwangju, Korea
(82) 62-530-3420
yckim@chonnam.ac.kr

Guee-Sang Lee
Chonnam National University
300 Yongbong-Dong street, Bukgu
500-757, Gwangju, Korea
(82) 62-530-3420
gslee@jnu.ac.kr

ABSTRACT

In this paper, we propose a novel segmentation algorithm for color images. This method is a combination of edge information with region information and a geometric active contour without re-initialization, called distance regularized level set evolution. The information given by a new edge detector using morphological gradient is more accurate than normal gradient computing methods for color images. And the information of the region containing objects is relied on Chan-Vese minimal variance criterion. With both of these information, the model can have its initial contour that is more flexible to construct anywhere, fast to evolve and quite exact to stop at the boundary of objects. The suggested algorithm has been applied on natural color images with good performance. Some experimental results have shown to compare our model with others with respect to accuracy and computational efficiency.

Categories and Subject Descriptors

I.4.6 [Image Processing and Computer Vision]: Segmentation – edge and feature detection, region growing, partitioning.

General Terms

Algorithms.

Keywords

Color images, active contour, morphological gradient, squared local contrast.

1. INTRODUCTION

Recently, research of image processing and computer vision on segmentation becomes an important problem. It has been applied widely into many applications. This is a fundamental step in object recognition, image compression, etc. because it simplifies the understanding of the image from thousands of pixels to a few regions which have same particular characteristics. Nowadays, the subject of color image segmentation has gained more and more

attention since they express a lot of information about objects in a scene than gray-scale images [1]. There has been a remarkable growth in the number of algorithms in the last decade. They can be considered in three main classes: feature-, image- and physics-based techniques. Most of them use color information and need some prior instructions to control their progress such as the number of clusters, the markers, the seeds, etc. as inputs of k-mean clustering, watershed, region-growing method, etc. respectively. In practice, their results are usually over-segmented due to noise or local irregularities. On the other hand, segmentation may also be obtained automatically by another like active contours or snakes. It uses the edge information which is easily found by approximating the gradient or the Laplacian of an image. Combining with region information and defined forces, this method returns resulting boundaries which can be insensitive to disturbances due to shadowing, highlights, or even noise. Because of advantages of active contour models, it is potential to be chosen for segmenting objects in color images. Figure 1 shows the results got by different segmentation methods.

For segmenting dynamic shapes of objects in the image, Kass, Witkins, and Terzopoulos [2] introduced active contours in 1987. It is also called snakes or deformable models defined as curves or surfaces. The contour can move to the boundary of the object under the influence of forces as constraints from the image within the image domain. Snake models have been applied to many applications despite few problems associated with its initialization and poor convergence to boundary concavities. After that, in 1988 the level set method was introduced by Osher and Sethian [3] as the first time. Its basic idea is to describe an active contour as the zero level set of a level set function to control the evolution of this contour for reaching the final boundary of objects by various external forces, such as gradient or gradient vector flow of the image, embedded in a speed function [4,5,6,7,8,9]. So, active contours can be grouped into two types: parametric and geometric active contours. The parametric deformable models are explicitly represented as parameterized curve in Lagrange formulation. While the geometric deformable models are represented implicitly and deform according to the Euler formulation based on the theory of evolution and geometric flows [1]. There are expected advantages of geometric active contours implemented through level set methods. One of them is to be suitable for handling complex and changeable topology, such as splitting and merging a contour. Another is its ability to perform numerical computations on Cartesian grid without concerning the parameterization of points on a contour.

Permission to make digital or hard copies of all or part of this work for personal or classroom use is granted without fee provided that copies are not made or distributed for profit or commercial advantage and that copies bear this notice and the full citation on the first page. To copy otherwise, or republish, to post on servers or to redistribute to lists, requires prior specific permission and/or a fee.

ICUIMC'12, February 20–22, 2012, Kuala Lumpur, Malaysia.
Copyright 2012 ACM 978-1-4503-1172-4...\$10.00.

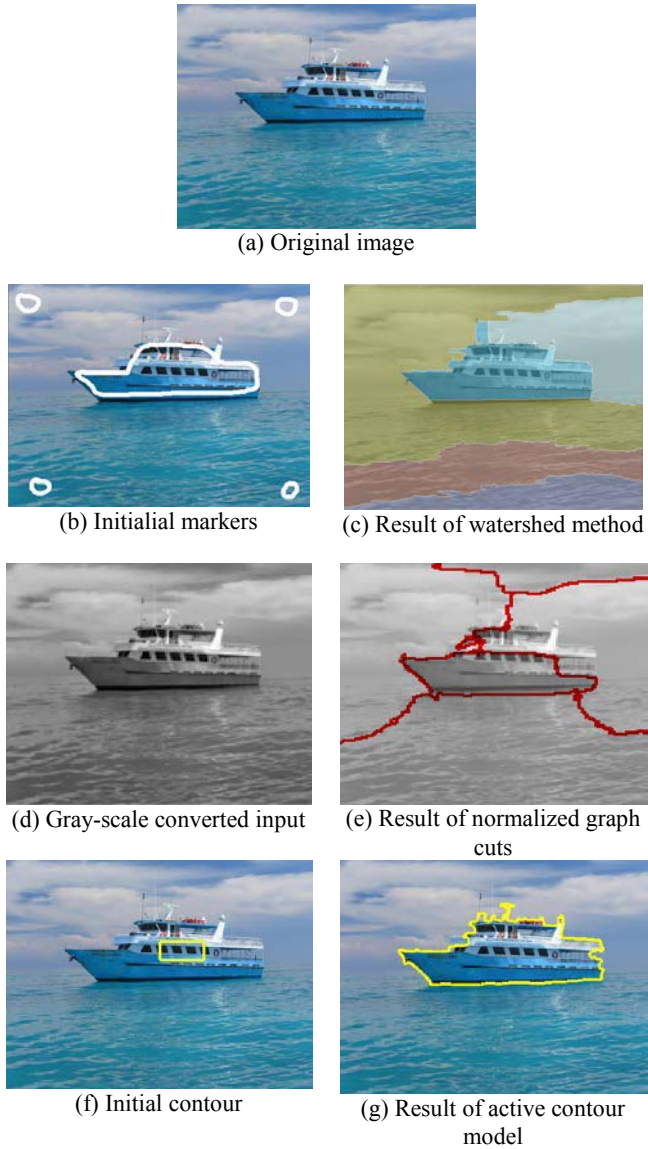


Figure 1. Boat segmentation by different segmentation algorithms

The quantitative shape description of an object, however, is more difficult to identify its exact locations. And the use of feature measurements to segment an image into meaningful areas of images can be driven by various criteria, such as edge, color, texture, or motion information. Numerous edge-based and region-based shape description methods have been employed for gray-scale images. Among these above criteria, edge information is used the most by computing many types of gradient values to identify the intensity changes appearing at edges or corners in images. But gradient-based measure of edges for gray-scale images can cause some difficulties in applying geometric active contour models to color image segmentation. Combining the edge-based models with different region-based information cues has led to powerful active contours for color images. The Geodesic-Aided C-V (GACV) method is a typical example. One more example is color-texture image segmentation by augmenting region and photometric invariant edge information model [10].

In this paper, we propose a combination of edge information and region information. This model modifies the idea of DRLSE

algorithm [11,12], an edge-based shape detector, to improve the segmenting results for flexibly initialized contour on color images. Its energy functional is represented by three parts: a level set regularization term, an external energy changed for the use of morphological gradient computed from a squared local contrast based image, and the supplementation of the Chan-Vese minimal variance criterion.

The outline of this paper is as follows. In Section II, a necessary background of level set method is provided together with a briefly introduction of distance regularized level set evolution (DRLSE) algorithm. Section III describes our improvements of DRLSE for color images. It includes morphological gradient, squared local contrast as well as minimal variance criterion. The experimental results of applying our proposed model to different color images are given in section IV. Finally, section V is conclusions to summarize and remark our work.

2. DISTANCE REGULARIZED LEVEL SET EVOLUTION

In image processing applications, the basic idea in active contour models is to evolve a curve, subject to constraints from a given image, in order to detect objects in that image [8]. Let Ω is a bounded open subset of \mathbb{R}^2 , with $\partial\Omega$ its boundary. Let $I: \overline{\Omega} \rightarrow \mathbb{R}$ be a gray level image. Early active contours (or fronts) are modeled as a dynamic parametric active contour $C(s,t): [0,1] \times [0,\infty) \rightarrow \mathbb{R}^2$ with a spatial parameter s as the points in the contour, and a temporal parameter t .

The level set method is basically represented by formulating an active contour $C(s,t)$ on the plane as the zero level set of a higher dimensional function $\phi(\vec{x},t)$, called level set function (LSF), in the space of \mathbb{R}^3 . Its differential equation can be described as

$$\frac{\partial \phi}{\partial t} + F|\nabla \phi| = 0 \quad (1)$$

$$\phi(x,y,t=0) = \phi_0(x,y)$$

where the set $\{(x,y) | \phi_0(x,y) = 0\}$ defines the initial contour. The function F is called a speed function and controls the motion of the contour. For image segmentation, this can be separated into two terms, an internal term which smoothens out the contour in areas of high curvature and an external term which forces the contour toward the desired object boundaries based on image data. To improve the highly imprecise computation made by some problems of the traditional level set method during the evolution [6,7], the function ϕ is initialized as a signed distance function

$$\phi(\vec{x},t) = \begin{cases} -d(\vec{x}) & \text{inside } C \\ 0 & \text{on } C \\ d(\vec{x}) & \text{outside } C \end{cases} \quad (2)$$

where $d(\vec{x}) = \min(|\vec{x} - \vec{x}_i|)$ for all \vec{x}_i on the contour C . Although this scheme gives good results due to its main property $|\nabla \phi| = 1$, it still has some disadvantages such as periodically complex re-initialization process, expensive computation and undesirable side effects of moving the zero level set away from its original location [10]. To overcome this problem, an algorithm named distance regularized level set evolution was introduced by Li et al. in [11].

Its general idea is to present a new variational formulation that forces the level set function to be close to a signed distance function, and therefore completely eliminates the need of the costly re-initialization procedure [1]. In this method, the energy functional was introduced as follows

$$\varepsilon(\phi) = \mu R_p(\phi) + \varepsilon_{ext}(\phi) \quad (3)$$

where $R_p(\phi)$ is the level set regularization term to characterize how close the level set function ϕ is to a signed distance function, μ is a constant controlling this deviation, and $\varepsilon_{ext}(\phi)$ is a certain external term depending on the desired image feature.

The regularization term can be seen as an internal energy term which penalizes the deviation of ϕ from a signed distance function during its evolution and defined as

$$R_p(\phi) = \int_{\Omega} p(\nabla \phi) dx \quad (4)$$

where p is chosen as a double-well potential function [12] provided by the below construction

$$p(s) = \begin{cases} \frac{1}{(2\pi)^2} (1 - \cos(2\pi s)) & \text{if } s \leq 1 \\ \frac{1}{2} (s - 1)^2 & \text{if } s \geq 1 \end{cases} \quad (5)$$

This potential $p(s)$ has two minimum points at $s=0$ to keep the LSF as a constant, with $|\nabla \phi| = 0$, at locations far away from the zero level set and $s=1$ to maintain the main property of signed distance function $|\nabla \phi| = 1$ only in a vicinity of the zero level set.

The external energy term in Eq. (3) is defined as

$$\varepsilon_{ext}(\phi) = \lambda \int_{\Omega} g \delta(\phi) |\nabla \phi| dx + \nu \int_{\Omega} g H(-\phi) dx \quad (6)$$

where $\lambda > 0$ and $\nu \in \mathfrak{R}$. Besides, g is an edge indicator function which will be described below. H is the Heaviside function, and δ is the univariate Dirac function defined by $\delta(\phi) = H'(\phi)$. In this term, the first component computes the length of the zero level contour of ϕ . This energy is minimized when the zero level contour of ϕ is located at the object boundaries. And the second component computes the weighted area of the region inside the contour ϕ as well as is able to speed up the motion of the zero level contour of ϕ .

By taking the derivative of the level set function with respect to t , or the negative value of the Gateaux derivative of the functional ε , the energy functional $\varepsilon(\phi)$ can be minimized by solving the following gradient flow

$$\frac{\partial \phi}{\partial t} = - \frac{\partial \varepsilon}{\partial \phi} \quad (7)$$

This equation can be written by calculus of variations [13] as

$$\frac{\partial \phi}{\partial t} = \mu \left(\Delta \phi - \operatorname{div} \left(\frac{\nabla \phi}{|\nabla \phi|} \right) \right) + \lambda \delta(\phi) \operatorname{div} \left(g \frac{\nabla \phi}{|\nabla \phi|} \right) + \nu g \delta(\phi) \quad (8)$$

3. A NOVEL NON-PARAMETRIC ACTIVE CONTOUR MODEL

A disadvantage of color image segmentation is that it is difficult to detect real boundaries of objects. Since these boundaries can be weak to distinguish, the colors describing objects and background are inhomogeneous, or the gradient-based edge detector cannot represent the boundary characteristics as well as control the effects of colors in the image. Thus, a novel combination is considered to increase the ability of edge detection to overcome its weakness.

3.1 Morphological Gradient based Edge Detector

Several types of gradient are used in color image processing to detect edges. One of them is called the morphological gradient. It is one simple combination of two basic operators of mathematical morphology that depend on the size and shape of the chosen structuring element. Using a flat structuring element at each point, the morphological gradient yields the difference between the maximum and the minimum values over the neighborhood at the point determined by the flat structuring element. In terms of mathematical morphology, it shows the difference between the dilation and the erosion operators of a given image [1].

The problem is that how a color image can be an input of morphological operators. As we known, color space is the way in which colors are expressed. In digital images, RGB color space is widely used the most. The edge detection in color images seems easier for human eyes since there are much more dissimilarity information. However, the design of image processing tools to enhance edges in color images is much more complex [14]. To detect them, the original method is to transform a color image to a scalar image. However, converting RGB color images into gray-scale ones can obtain negative effects. Some information to distinguish different colors can be lost if they have the same gray value. In this case, sometimes the boundary between objects and background cannot be separated clearly. Thus, in [15], Cumani et al. gave an edge definition based on a computing method which is called squared local contrast. The RGB color of each pixel is treated as a 3D vector, and the strength of the edge is the magnitude of the maximum gradient.

Let us consider a color image as a two-dimension vector field $I(x,y)$ with three components R, G and B. In this case, the squared norm of the directional derivative of I in the direction of the unit vector $\vec{a} = (a_1, a_2)$ named the squared local contrast $S(P; \vec{a})$ of point $P(x,y)$ is defined as below:

$$S(P; \vec{a}) = \frac{\partial I}{\partial x} \cdot \frac{\partial I}{\partial x} \cdot a_1 \cdot a_1 + 2 \cdot \frac{\partial I}{\partial x} \cdot \frac{\partial I}{\partial y} \cdot a_1 \cdot a_2 + \frac{\partial I}{\partial y} \cdot \frac{\partial I}{\partial y} \cdot a_2 \cdot a_2 \quad (9)$$

$$= E \cdot a_1^2 + 2 \cdot F \cdot a_1 \cdot a_2 + G \cdot a_2^2$$

Here

$$E = \frac{\partial I}{\partial x} \cdot \frac{\partial I}{\partial x} = \sum_{i=1}^3 \frac{\partial I_i}{\partial x} \cdot \frac{\partial I_i}{\partial x}$$

$$F = \frac{\partial I}{\partial x} \cdot \frac{\partial I}{\partial y} = \sum_{i=1}^3 \frac{\partial I_i}{\partial x} \cdot \frac{\partial I_i}{\partial y}$$

$$G = \frac{\partial I}{\partial y} \cdot \frac{\partial I}{\partial y} = \sum_{i=1}^3 \frac{\partial I_i}{\partial y} \cdot \frac{\partial I_i}{\partial y} \quad (10)$$

The eigenvalues of the following matrix $M = \begin{pmatrix} E & F \\ F & G \end{pmatrix}$ coincide

with the extreme values of $S(P; \bar{a})$ and are attained when \bar{a} is corresponding eigenvectors [10]. The extreme values are

$$\lambda_{\pm} = \frac{E+G}{2} \pm \sqrt{\frac{(E-G)^2}{4} + F^2} \quad (11)$$

In this paper, we use

$$f_{edge} = \lambda_+ - \lambda_- \quad (12)$$

as an input to calculate the morphological gradient, $\nabla_B(f_{edge})$, given by:

$$\nabla_B(f_{edge}) = \delta_B(f_{edge}) - \varepsilon_B(f_{edge}) \quad (13)$$

where δ and ε are, respectively, the morphological dilation and erosion, and $B \subset E$ is the structuring element of those operators.

The result is an image in which each pixel value indicates the contrast intensity in the close neighborhood of that pixel, or containing the maximum difference of gray level inside the structuring element B . And the gradient peaks are located on the edges.

Finally, the above morphological gradient is used to be a stopping function for color image as

$$g_{color} = \frac{1}{1 + \nabla_B(f_{edge})} \quad (14)$$

3.2 Chan-Vese Minimal Variance Criterion

The Chan-Vese model uses the region statistic information and has the advantage of the region model. A strong point when incorporating region-based information into an energy functional as an additional constraint is that this model has much larger convergence range and the initialization of the curve can be anywhere in the image [16]. The proposed idea by Chan et al. in [8] can be shown briefly as figure 2.

The Chan-Vese minimal variance criterion, or sometimes called the fitting term, is given by

$$F_1(C) + F_2(C) = \int_{inside C} (I - c_1)^2 dx dy + \int_{outside C} (I - c_2)^2 dx dy \quad (15)$$

where C is any other variable curve, and the optimal c_1 , c_2 , depending on C , are the averages of I inside C and respectively outside C . If the curve C is exactly on object boundary, then $F_1(C) \approx 0$, $F_2(C) \approx 0$, and the fitting term is minimized.

By taking the derivative of Eq. (15) with respect to the curve C , the first variation is

$$\begin{aligned} \frac{\partial F_1}{\partial C} + \frac{\partial F_2}{\partial C} &= -(I - c_1)^2 + (I - c_2)^2 n \\ &= (c_1 - c_2)(2I - c_1 - c_2)n \end{aligned} \quad (16)$$

where n denotes the exterior normal to the boundary C .

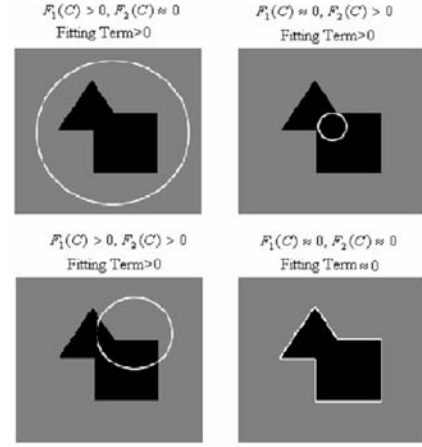


Figure 2. All possible cases in position of the curve

3.3 Modified Distance Regularized Level Set Evolution for Color Images

As Eq. (8), the original distance regularized level set evolution (DRLSE) uses the edge information to stop its evolution when catching the boundaries of objects. This approach seems only good in the case that its initial contour is inside or outside the object completely. To let DRLSE be suitable for cases where a contour is initialized flexibly, the region information is added as a constraint. Thus, according to the Chan-Vese minimal variance criterion mentioned above, we propose a new model that can use both two types of information.

$$\begin{aligned} \frac{\partial \phi}{\partial t} &= \mu \left(\Delta \phi - \operatorname{div} \left(\frac{\nabla \phi}{|\nabla \phi|} \right) \right) + \lambda \delta(\phi) \operatorname{div} \left(g_{color} \frac{\nabla \phi}{|\nabla \phi|} \right) + v g_{color} \delta(\phi) \\ &\quad + w \delta(\phi) (c_1 - c_2) (2g_{color} - c_1 - c_2) \end{aligned} \quad (17)$$

This new model can shorten the evolution time and we call it the new active contour for color image segmentation. c_1 , c_2 are the average intensities of g_{color} inside and outside the contour are computed as

$$\begin{aligned} c_1(\phi) &= \frac{\iint_{\Omega} g_{color} H(\phi) dx dy}{\iint_{\Omega} H(\phi) dx dy} \\ c_2(\phi) &= \frac{\iint_{\Omega} g_{color} (1 - H(\phi)) dx dy}{\iint_{\Omega} (1 - H(\phi)) dx dy} \end{aligned} \quad (18)$$

Here the Heaviside function is $H(\phi) = \begin{cases} 1, & \text{if } \phi \geq 0 \\ 0, & \text{if } \phi < 0 \end{cases}$ and the one-dimensional Dirac measure $\delta(\phi) = H'(\phi)$. Especially, in this model, we use the energy image g_{color} to calculate the region information rather than the original image like usual.

4. EXPERIMENTAL RESULTS

In practice, to implement Eq. (17) in numerical scheme, the univariate Dirac function and Heaviside function in the external energy term are approximated by the following smooth functions defined by

$$\delta_\varepsilon(x) = \begin{cases} \frac{1}{2\varepsilon} \left[1 + \cos\left(\frac{\pi x}{\varepsilon}\right) \right] & |x| \leq \varepsilon \\ 0 & |x| > \varepsilon \end{cases} \quad (19)$$

$$H_\varepsilon(x) = \begin{cases} \frac{1}{2} \left[1 + \frac{x}{\varepsilon} + \frac{1}{\pi} \sin\left(\frac{\pi x}{\varepsilon}\right) \right] & |x| \leq \varepsilon \\ 1 & x > \varepsilon \\ 0 & x < -\varepsilon \end{cases} \quad (20)$$

where ε is a constant chosen by implementing experiment. We use $\varepsilon = 1.5$ for all experiments in this paper.

The initial function ϕ_0 can be replaced as a signed distance function or a binary step function defined by

$$\phi_0(x) = \begin{cases} -c_0 & \text{if } x \in R_0 \\ c_0 & \text{otherwise} \end{cases} \quad (21)$$

where R_0 is a region in image domain and $c_0 > 0$ is a constant. Then, the discretization of evolution equation (17) is followed by the forward difference scheme to express the below difference equation

$$\phi_{i,j}^{k+1} = \phi_{i,j}^k + \tau L(\phi_{i,j}^k) \quad (22)$$

where $L(\phi_{i,j}^k)$ is the approximation of the right hand side in Eq. (17) by the spatial difference scheme approximated by the central difference for partial derivatives and the forward difference for temporal derivative.

To demonstrate the performance of the new geometric active contour model for color image segmentation, we have carried out various types of images as well as several comparison experiments between our models and others. A PC equipped with Intel(R) Core(TM)2 CPU 6700 @2.66GHz 2.67GHz and 2GB RAM is used to run in environment of Matlab 2011a. And our method has been applied to various real natural images of the Berkeley Segmentation Data Set 500 at [17]. The zero level set contours in all following figures are described by a red or yellow curve bounding the object.

Figure 3 shows the results of our new geometric active contour models combining edge information and region information after applying to a 481x321 image with 500 iterations. In this image, we used the parameters $\mu = 0.02$, $\lambda = 5$, $\nu = 3$, $w = 0.1$ and time step $\tau = 10$. Figure 3(a) is the original image. The initial zero level set ϕ is represented in red rectangle in figure 3(b). All figures 3(c), (d) and (e) are the results get from this new model after 100, 300 and 500 steps of evolution and they take approximately 14.8, 45.1 and 81.9 seconds respectively. The final contour which describes the extracted object is shown by white curve in figure 3(f). This resulting contour is quite smooth and closes the true boundary of the object in the image.

The intermediate steps to reach the segmenting result in figure 3 include squared local contrast based computation of the given color image and morphological gradient calculation. Their results are shown in figure 4 below.

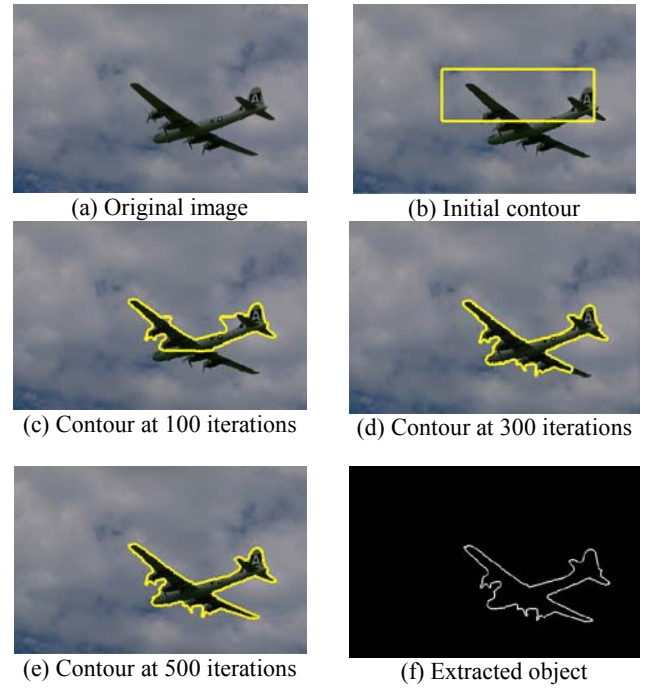


Figure 3. Evolution of the zero level set and the final extracted result for a color image

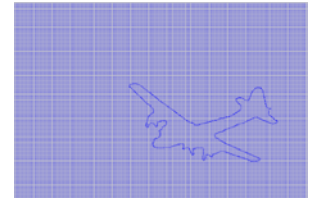
In figure 4, the results of edge detection for color images are accurate enough to be an input of the segmentation process. Figure 4(a) shows a good outcome to enhance the essential boundary of the object inside the given image. And morphological gradient operator applied to take the maximum difference of gray level inside a flat disk-shaped structuring element transforms figure 4(a) into 4(b). Its calculated gradient value can also be displayed by the magnitude and orientation of gradient vectors at each pixel in the image as figure 4(c).



(a) Squared local contrast



(b) Morphological gradient transform



(c) Gradient image

Figure 4. Intermediate results of the segmentation process

Next, figure 5 indicates the relative locations of the initialization of this model to the object since its initial contour can be positioned flexibly in the image. So that there are three cases of study including completely outside, inside and cutting across the object which we need to segment in an image. These case are correlative to figure 5(a), (c) and (e) respectively. Despite of their locations in the image, the active contours still deform and move

towards the boundary of the object given by the gradient value. And all segmentation results of three cases in figure 5(b), (d), and (f) are similar to each other.

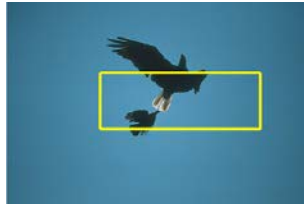
Color images with the initial contour	Segmentation results
	
(a) Completely outside	
	
(c) Completely inside	
	
(e) Cutting across	

Figure 5. Segmentation from different positions of the initial contour with respect to the object

Figure 6 show the comparison of experimental results by using variety of deformable models such as our new active contour model, RGAC model in [1], localizing region based active contour (LRAC) in [18], and Chan-Vese model in [19] for color images. With each models, the initial contours are generated as figure 6(b), (d), (f) and (k) respectively. Corresponding to their initialization, the segmentation results are reached. As looking at the figure 6, results indicate that our model performs in a much superior way. Figure 6(c) shows that our active contour model can get the correct boundary of the object after 400 steps of evolution which take 35.4 seconds. This contour is very smooth with respect to the boundary of this airplane object. Conversely, RGAC model can give the final contour as figure 6(e) after 250 iterations during 29.7 seconds. This model runs faster than our model but its result is not smooth even when we increase the number of steps of evolution. The result in figure 6(g) belongs to localizing region based active contour model. It takes 223.5 seconds after 3000 steps of evolution. But the model cannot get the correct segmentation result with the same initial contour as the figure 6(b). The final figure 6(l) is the result of vector valued Chan-Vese model. Its initial contour is created, deformed and stopped automatically after 800 steps of evolution which take 37.9s. So, the results show that our method is better than the Chan-Vese

model as well as more effective and faster than the LRAC model since it transforms the color image into the gray-scale image before the evolution. This color space transformation can cause an information loss of the image.

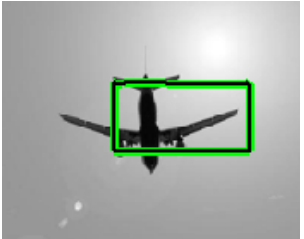
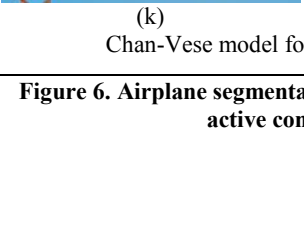
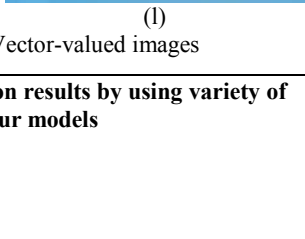
Color images with the initial contour	Segmentation results
	
(a) Original color image	
	
(b) Our new active contour models	
	
(d) RGAC model	
	
(f) Localizing region based active contour	
	
(k) Chan-Vese model for Vector-valued images	
	
(l)	

Figure 6. Airplane segmentation results by using variety of active contour models

Figure 7 is given by trying our new active contour model in various types of color images. To have a good performance of this model, there should be some assumptions. Firstly in all color images, the difference of color intensity between the segmented objects and the background is large enough to be able to distinguish mutually. Next, the colors of the objects or the background in the image should be nearly homogeneous. This figure also shows a weak point of our method which we should improve. That is the model can only segment all objects in an image as one group. It means that our model does not separate them into different ones from each other. For an example, figure 7(c) has flowers and one butterfly. The target should be segmented this image into three parts which are background, flowers, and the butterfly. However, the segmented result is just one object including both flowers and the butterfly as figure 7(d).

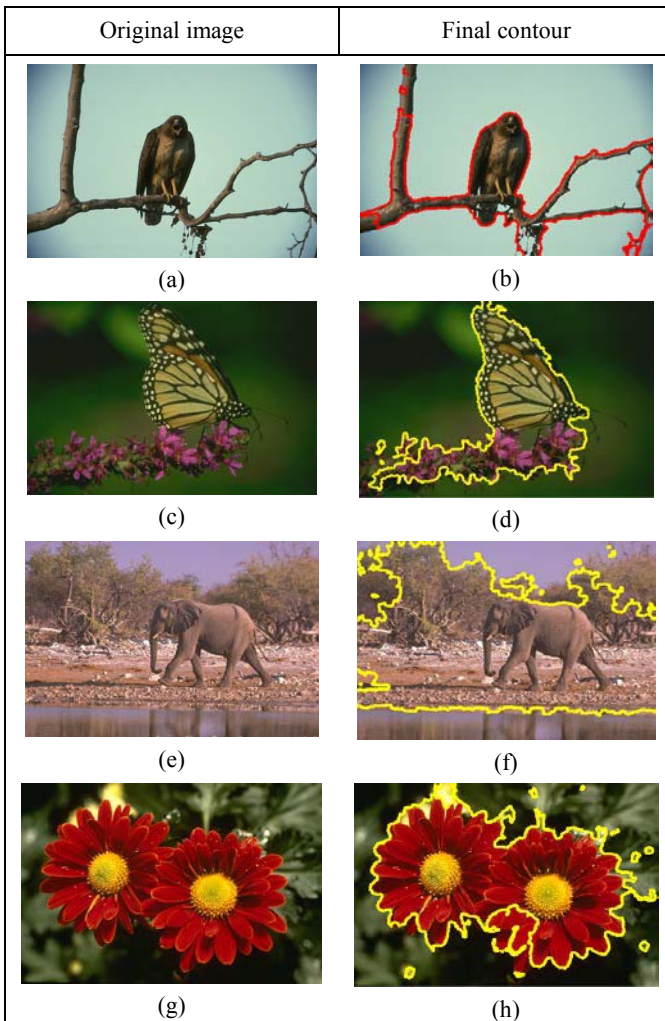


Figure 7. Results of our model with various types of color images

5. CONCLUSIONS

Color image segmentation is an interesting problem which attracts many attentions nowadays. In order to solve it, in this paper, we proposed a novel geometric active contour model combining morphological gradient of a squared local contrast image with distance regularization method for color images. By using not only edge information but also region information of color images,

in this model, a closed initial curve can find the boundary of the objects smoothly and exactly. Its performance has been showed to be more acceptable in terms of accuracy and efficiency than other deformable models. Its computational time is also decreased considerably. However, this model still has some limitations that we have to assume in the experiment session. Our future work is to continue concentrating on color image segmentation with a reduction of assumptions to reach better results for natural color images.

6. ACKNOWLEDGMENTS

This research was supported by Basic Science Research Program through the National Research of Korea (NRF) funded by the Ministry of Education, Science and Technology (2011-0006109) and by Basic Science Research Program through the National Research of Korea (NRF) funded by the Ministry of Education, Science and Technology (2011-0029429).

7. REFERENCES

- [1] HaiJun Wang, Ming Liu, and WenLai Ma 2010. Color Image Segmentation Based on a New Geometric Active Contour Model. In *IEEE International Conference on Machine Vision and Human-machine Interface*, pp. 6-9.
- [2] M. Kass, A. Witkin, and D. Terzopoulos 1987. Snakes: active contour models. In *International Journal of Computer Vision*, Vol. 1, pp. 321-331.
- [3] S. Osher and J. Sethian 1988. Fronts propagating with curvature-dependent speed: Algorithms based on Hamilton-Jacobi formulations. In *Journal of Computational Physics*, Vol. 79, pp. 12-49.
- [4] V. Caselles, R. Kimmel, and G. Sapiro 1997. Geodesic active contours. In *International Journal of Computer Vision*, Vol. 22(1), pp. 61-79.
- [5] C. Xu and Jerry L. Prince 1997. Gradient vector flow: A new external force for snakes. In *IEEE Proceedings of Conference on Computer Vision and Pattern Recognition*, CVPR'97, pp. 66-71.
- [6] S. Osher and R. Fedkiw 2003. *Level set methods and Dynamic implicit surfaces*. In Springer, New York.
- [7] J. A. Sethian 1999. *Level set methods and Fast marching methods*. In Cambridge University Press, Cambridge.
- [8] Tony F. Chan and Luminita A. Vese 2001. Active contours without edges. In *IEEE Transactions on Image Processing*, Vol. 10, No. 2 (Feb. 2001), pp. 266-277.
- [9] Wei-gang Chen 2006. Gradient vector flow using an implicit method. In *International Journal of Information Technology*, Vol. 12, No. 2, pp. 14-23.
- [10] Zheng Ying, Li Guangyao, Sun Xiehua, and Zhou Xinmin 2009. A geometric active contour model without re-initialization for color images. In *Image and Vision Computing* 27 (2009), pp. 1411 – 1417.
- [11] Chunming Li, Chenyang Xu, Changfeng Gui, and Martin D. Fox 2005. Level Set Evolution Without Re-initialization: A New Variational Formulation. In *Proceedings of the 2005 IEEE Computer Society Conference on Computer Vision and Pattern Recognition*. CVPR'05, Vol 1, pp. 430-436.

- [12] Chunming Li, Chenyang Xu, Changfeng Gui, and Martin D. Fox 2010. Distance regularized level set evolution and its application to image segmentation. In *IEEE Transactions on Image Processing*, Vol. 19, No. 12 (December 2010), pp. 3243-3254.
- [13] L. Evans 1998. *Partial Differential Equations*. In Providence: American Mathematical Society.
- [14] R. Hirata Jr., F. C. Flores, J. Barrera, R. A. Lotufo, and F. Meyer 2000. Color Image Gradients for Morphological Segmentation. In *IEEE Proceedings of SIBGRAPO'2000* (Gramado, Brazil), pp. 316-322.
- [15] A. Cumani 1991. Edge detection in multi-spectral images. In *CVGIP: Graphical Models and Image Processing* 53(1), pp. 40-51.
- [16] B. V. Dhandra and R. Hegadi 2007. Active Contours without Edges and Curvature Analysis for Endoscopic Image Classification. In *International Journal of Computer Science and Security*, Volume (1): Issue (1), pp. 19-32.
- [17] <http://www.eecs.berkeley.edu/Research/Projects/CS/vision/>
- [18] S. Lankton and A. Tannenbaum 2008. Localizing Region-based Active Contours. In *IEEE Transactions on Image Processing*, Vol. 17, No. 11 (November 2008), pp. 2029-2039.
- [19] T. F. Chan, B. Y. Sandberg, and L. A. Vese 2000. Active Contours without Edges for Vector-Valued Images. In *Journal of Visual Communication and Image Representation* 11, pp. 130-141.